analytical chemistry

Article

pubs.acs.org/ac

Surface-Based and Mass Spectrometric Approaches to Deciphering Sugar–Protein Interactions in a Galactose-Specific Agglutinin

Carmen Jiménez-Castells,[†] Sira Defaus,[†] Adrian Moise,[‡] Michael Przbylski,[‡,*] David Andreu,*[,†] and Ricardo Gutiérrez-Gallego*[,†,§]

[†]Department of Experimental and Health Sciences, Pompeu Fabra University, Barcelona Biomedical Research Park, 08003 Barcelona, Spain

[‡]Department of Chemistry, University of Konstanz, 78457 Konstanz, Germany

[§]Bio-analysis group, Neuroscience Research Program, IMIM-Parc Salut Mar, Barcelona Biomedical Research Park, 08003 Barcelona, Spain

ABSTRACT: Interest in powerful, nanosized tools to analyze in detail glycan–protein interactions has increased significantly over recent years. Here, we report two complementary approaches to characterize such interactions with high sensitivity, low sample consumption, and without the need for sample labeling, namely, surface plasmon resonance (SPR) and an approach that combines limited proteolysis and mass spectrometry. Combination of these two approaches to investigate glycan–protein interactions allows (1) to characterize interactions through kinetic and thermodynamic parameters, (2) to capture efficiently the carbohydrate-binding protein, and (3) to identify the interacted protein and its carbohydrate binding site by mass spectrometry. As a proof of principle, the interaction of the galactose-specific legume lectin *Erythrina cristagalli* agglutinin with several sugars has been characterized in-depth by means of these two approaches.

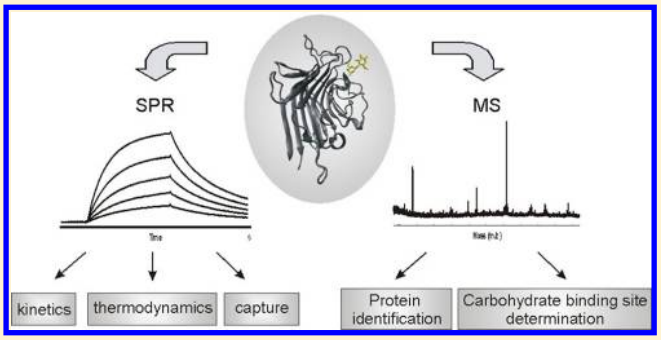

In recent years the interest in exploring carbohydrate–protein interactions has soared as their decisive role in many biological processes, for example, pathogen–host cell adhesion,[1] metastasis,[2] or fertilization,[3] became evident. Although it is estimated that over 50% of all proteins are glycosylated,[4] and that these glycans play key roles in all sorts of communication processes, little is known about their binding partners. Several techniques for screening interaction partners, mostly focused on protein–protein binding, have been developed, including tandem affinity purification[5] or two-hybrid screening.[6] More recently, surface plasmon resonance (SPR) has also been employed to capture new binding partners prior to characterization by mass spectrometry[7] or HPLC profiling.[8] In this approach one of two interacting entities is immobilized onto the surface of a sensor chip and its partner is flown over. Unlike other techniques, SPR provides both quantitative and qualitative interaction data, in real time and under conditions closely mimicking physiological ones. Although originally designed for protein–protein studies,[9] soon it was applied in other contexts, for example, DNA–protein,[10] sugar–protein,[11] and lipid–protein interactions.[12] While SPR-based biosensors are mostly used to determine kinetic rate constants, thermodynamic data can also be obtained by determining equilibrium constants within a given temperature range.[13] Moreover, some instrumental designs incorporate sample recovery features that allow to combine interaction analysis with MS identification.[14] In the particular case of sugar–protein interactions, we have devised a reliable method for immobilizing glycan-displaying probes on SPR chips.[15] In this approach, the sugar moiety is immobilized through a tailor-made peptide module on the sensor surface and the interacting lectin is passed over. The oxime ligation chemistry is used to attach the glycan via the aminooxy functionality (Aoa) to the peptide module, Aoa-GFKKG-amide,[16] whereas the methylated version, *N*[Me]-O-Aoa-GFKKG-amide ensures correct exposure of the carbohydrate on the chip surface as well as the conformational integrity (e.g., as a pyranose ring) of the monosaccharide unit proximal to the surface, a particularly relevant point for short (mono- and disaccharide) epitopes.[17] The two Lys residues in the peptide module guide coupling to the carboxyl-functionalized sensor surface, previously activated as *N*-hydroxysuccinimide ester.

For detailed structural information on lectin–glycan interactions, well-established techniques, such as X-ray crystallography[18] and NMR spectroscopy,[19] require amounts of both partners in the milligram range and purity levels not often easily achievable. Recently, a novel approach combining proteolytic digestion of protein–glycan complexes and mass spectrometry (CREDEX-MS, carbohydrate recognition domain excision mass spectrometry)[20,21] has demonstrated its efficiency

Received: March 19, 2012
Accepted: July 3, 2012
Published: July 3, 2012

   dx.doi.org/10.1021/ac300766z | *Anal. Chem.* 2012, 84, 6515–6520

in the identification and structural definition of carbohydrate binding sites. In this approach, the carbohydrate is coupled to a divinylsulfone-activated Sepharose support and the lectin-containing specimen is bound to it under controlled conditions. The carbohydrate-lectin complex is then digested with specific proteases and, after washing-off non-interacting fragments, the binding peptides are eluted and subsequently identified by MS. Like in all MS techniques the sample amount requirements are substantially lower (micrograms vs milligrams) than for X-ray crystallography or NMR.

Here we describe how the combined use of SPR and CREDEX-MS, two nanosized complementary analytical methodologies, can provide detailed information on carbohydrate-lectin interactions. As an example, the interaction between the β-galactose-specific legume lectin *Erythrina cristagalli* agglutinin (ECA) and a series of related β-galactosides [Gal(β1−4)GlcNAc, Gal(β1−4)Glc, Gal(β1−3)-GlcNAc, and Gal(β1−6)GlcNAc) has been studied by both SPR and MS, and the carbohydrate-binding site of the lectin has been identified.

MATERIALS AND METHODS

Chemicals. Fmoc [N^{α}-(9-fluorenylmethyloxycarbonyl)]-protected amino acids were purchased from Senn Chemicals (Dielsdorf, Switzerland). The dicyclohexylamine (DCHA) salt of Boc (*tert*-butyloxycarbonyl)-methylaminooxyacetic acid was from NeoMPS (Strasbourg, France). 2-(1*H*-Benzotriazol-1-yl)-1,1,3,3-tetramethyluronium hexafluorophosphate (HBTU) was obtained from Iris Biotech (Marktredwitz, Germany). Rink amide MBHA resin was from Novabiochem (Läufelfingen, Switzerland). *N*,*N*-Diisopropylethylamine (DIEA) was from Merck Biosciences (Darmstadt, Germany), and triisopropylsilane was from Sigma-Aldrich (Madrid, Spain). HPLC-grade acetonitrile (ACN), *N*,*N*-dimethylformamide (DMF), trifluoroacetic acid (TFA), and diethyl ether were from SDS (Peypin, France). Disaccharides (Gal(β1−3,4,6)GlcNAc) were purchased from Dextra (Reading, United Kingdom). Lactose (Gal(β1−4)Glc) and lectin from *Erythrina cristagalli* (ECA) were from Sigma-Aldrich (Madrid, Spain). CM5 sensor chips, 1-ethyl-3-(3-diethylaminopropyl)-carbodiimide (EDC), *N*-hydroxysuccimide (NHS), and ethanolamine hydrochloride pH 8.5, were from BIAcore (GE Healthcare, Uppsala, Sweden), Sepharose-4B and divinylsulfone were purchased from Sigma-Aldrich (Madrid, Spain). Microcolumn and 35-μm pore size filters were from MoBiTec (Göttingen, Germany). Sequencing-grade modified porcine trypsin was from Promega (Madison, USA). Sequencing-grade chymotrypsin and Glu-C were from Roche Diagnostics GmbH (Penzberg, Germany). Poros 20 R2 was obtained from Applied BioSystems (Foster City, USA).

Peptide and Glycopeptide Synthesis. *N*[Me]-*O*-Aoa-GFKKG-amide[17] was synthesized by Fmoc-based solid-phase synthesis on a Rink MBHA resin (0.70 mmol/g). Boc-methylaminooxyacetic acid·DCHA (500 mg) was converted to the free carboxyl form by acid extraction with 0.1 M HCl and ethyl acetate (50 mL each). Manual couplings with 3 equiv each of Boc-amino acid and HBTU and 6 equivalent of DIEA were used for 1 h, r.t., in DMF. Resin cleavage and full deprotection were done with TFA−water−triisopropylsilane (95:2.5:2.5, v/v, 90 min, r.t.). Peptides were isolated by precipitation with cold *tert*-butyl-methyl ether and centrifugation, then solubilized in water and lyophilized. The synthetic product was >95% pure by analytical HPLC and had the correct mass by MALDI-TOF MS.

Conjugation of *N*[Me]-*O*-Aoa-GFKKG-amide to disaccharides was done at 20 and 25 mM, respectively in 0.1 M sodium acetate, at pH 3.5 for *N*Ac-disaccharides and pH 4.6 for lactose. After 72 h at 37 °C, the glycopeptides were purified by semipreparative HPLC on SphereClone C18 (Phenomenex, 250 × 10 mm; 5 μm) using a 10−20% linear gradient of acetonitrile into water (both eluents with 0.1% TFA). Glycopeptide-containing fractions were neutralized with 10 mM ammonium bicarbonate to prevent acid degradation and lyophilized. All disaccharide-*N*[Me]-*O*-GFKKG-amide glycopeptides had the expected mass by MALDI-TOF MS.

SPR Measurements. Experiments were performed on carboxymethyl-functionalized CM5 sensor chips in a Biacore 3000 instrument (Biacore SA, Uppsala, Sweden). In all experimental procedures the running buffer was HBS-P buffer supplemented with 5 mM $CaCl_2$ and 1 mM $MnCl_2$. For *N*[Me]-*O*-Aoa-GFKKG-amide immobilization, the surface was activated with 60 μL of a mixture of EDC (0.2 M) and NHS (0.05 M) in water, at 5 μL/min, then glycopeptides were passed at 1 mg/mL in 10 mM sodium acetate, pH 6, for 12 min, followed by a blocking step with 1 M ethanolamine·HCl, pH 8.5. As a reference surface, *N*[Me]-*O*-Aoa-GFKKG-amide was immobilized on a different flow channel.

For determination of kinetic parameters, several concentrations in the 66 nM−2.6 μM range were prepared by a set of 2/3-fold dilutions of the most concentrated sample in running buffer (10 mM HEPES, 25 mM sodium chloride, 5 mM calcium chloride, 1 mM manganese(II) chloride,[22] pH 7.4). Binding experiments were performed at 25 °C at two flow rates (10 and 50 μL/min). After lectin injection (3-min pulse), sample solution was replaced by running buffer and the dissociation phase was monitored for 6 min. Sensor surface was regenerated with a 50 μL-injection of 10 mM lactose. Two replicates were performed for each injection.

For thermodynamic experiments, five ECA concentrations (100, 250, 400, 550, and 700 nM) in running buffer were explored in the 10 to 25 °C interval, with 2.5 °C increments controlled by a Peltier device. Two replicates of each solution were injected (3-min pulse) over the *N*-acetyllactosamine-(lacNAc)-funcionalized and the reference surface at 50 μL/min. As in the kinetic experiments, after lectin injection sample injection was replaced by running buffer and the dissociation phase was monitored for 6 min. After each cycle, the sensor surface was regenerated with 50-μL injections of 25 mM lactose. In both kinetic and thermodynamic experiments, the specific binding response was obtained by subtracting form each channel the reference channel response. Curve fitting of the sensorgram curves was done with the BIAevaluation 4.0.1 software package.

For recovery experiments, a 1 μM solution of ECA was injected for 3 min at 10 μL/min over the lacNAc surface at 25 °C. By means of the MS recover function, captured material was eluted in a 2-μL volume of 10 mM lacNAc, concentrated by vacuum centrifugation and analyzed by MALDI-TOF MS.

CREDEX-MS. For disaccharide immobilization, 50 μg of dry divinylsulfonyl-activated Sepharose were treated with a solution of 5 mg of lacNAc in 50 μL of 0.5 M potassium carbonate, pH 11, overnight at r.t. The reaction mixture was poured into a microcolumn and washed sequentially with 50 mM ammonium acetate, pH 4, and 50 mM and ammonium bicarbonate, pH 8. The microcolumn was equilibrated with SPR running buffer and stored at 4 °C. For excision experiments, 20 μg of ECA in running buffer (75 μL) were loaded onto the lacNAc-Sepharose

dx.doi.org/10.1021/ac300766z | *Anal. Chem.* 2012, 84, 6515−6520

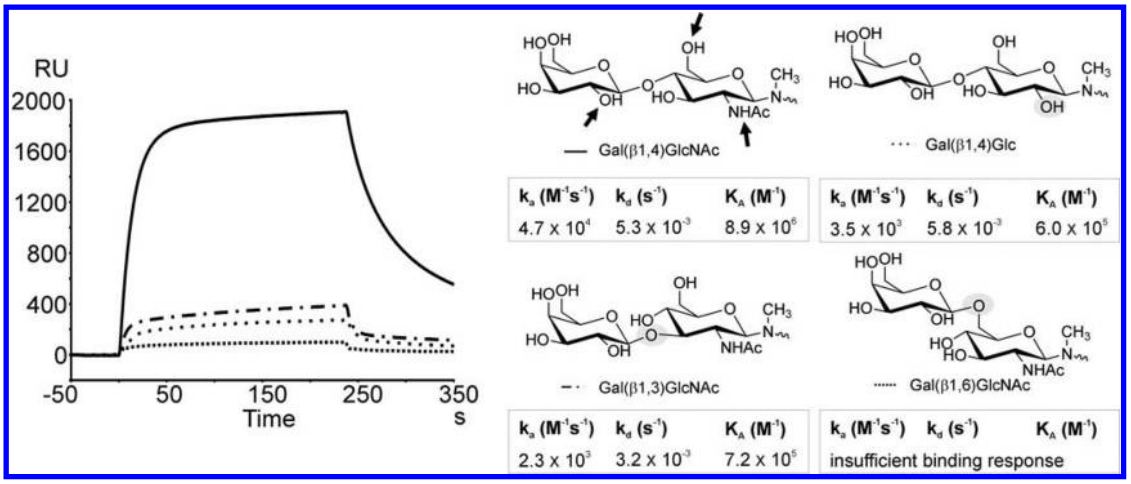

Figure 1. SPR analysis of ECA binding to four β-galactosides. Glycopeptide probes displaying the epitopes were coupled to the sensor surface at similar immobilization levels. The sensorgrams show the differential curves after subtracting a reference channel with no epitope immobilized. Gal(β1−4)GlcNAc functional groups crucially involved in ECA interaction are marked with an arrow. In the other disaccharide structures, functional groups whose modification causes loss of ECA affinity are shaded. The kinetic rate constants (k_a, k_d) and the derived affinity constant (K_A) of ECA to the four different glycoprobes exposing terminal β-galactosyl-disaccharides are provided in the boxes.

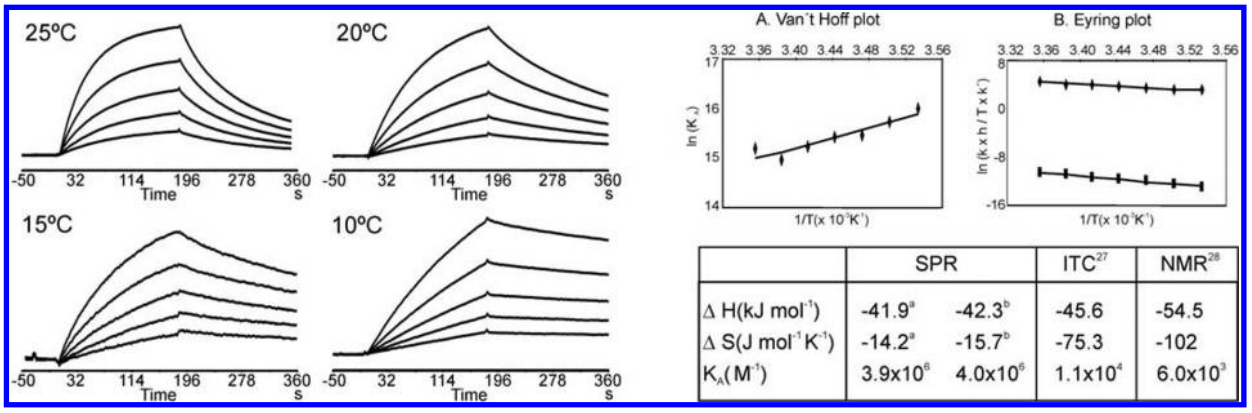

	SPR		ITC[27]	NMR[28]
Δ H(kJ mol^{-1})	-41.9[a]	-42.3[b]	-45.6	-54.5
Δ S(J mol^{-1} K^{-1})	-14.2[a]	-15.7[b]	-75.3	-102
K_A(M^{-1})	3.9x10^6	4.0x10^6	1.1x10^4	6.0x10^3

Figure 2. Left: SPR sensorgrams demonstrating the effect of temperature on the interaction between ECA and Gal-β1,4-GlcNAc. Top right: Van't Hoff plot for the binding of ECA to lacNAc. Dots showing affinity constants determined at 2.5 °C intervals in the 10−25 °C range could be linearly fitted to derive ΔH values. B. Eyring plots for the same interaction. Dots and squares correspond to association and dissociation rate constants, respectively; both series could be linearly fitted to derive ΔH values. Bottom right: Thermodynamic parameters for ECA-lacNAc interactions determined using SPR, ITC and NMR. In the SPR block the thermodynamic parameters derived from the (a) Van't Hoff or (b) Eyring equation.

microcolumn and incubated for 24 h at 37 °C, followed by washes with binding buffer. The sugar-lectin complex was then digested overnight with 1 μg trypsin in 75 μL of 25 mM ammonium bicarbonate, pH 8.5, 37 °C. Unbound digestion products were eluted and the column washed with running buffer. For chymotrypsin digestion, 1 μg enzyme in 75 μL of 100 mM Tris·HCl, 10 mM calcium chloride, pH 7.8, was added to the microcolumn and incubated for 24 h at 35 °C. After washes with running buffer, specific-bound peptides were eluted with 600 μL of acetonitrile−water (6:4; with 0.1% TFA), concentrated and lyophilized. Prior to analysis, digestion peptides were desalted on Poros R2 mini-columns packed in Geloader tips. MALDI-TOF MS measurements were carried out on a Voyager-DE STR workstation (Applied Biosystems) operating in the reflectron, positive polarity mode, with data processing by the Data Explorer Software (Applied Biosystems), or in a Bruker Biflex linear TOF mass spectrometer (Bruker Daltonik, Bremen, Germany) equipped with a nitrogen UV laser (λ_{max} 337 nm) and a XMASS data system for spectra acquisition and instrument control.

RESULTS AND DISCUSSION

Structural Insights from SPR Studies. The medium-throughput screening capacity of our Biacore 3000 instrument allowed simultaneous analysis of ECA binding to four β-galactoside-containing epitopes: Gal(β1−4)GlcNAc, Gal(β1−4)Glc, Gal(β1−3)GlcNAc, and Gal(β1−6)GlcNAc. Kinetic rate constants (k_a, k_d) for both association and dissociation phases, and the derived affinity constants (K_A) could be determined for the first three disaccharides (Figure 1); for Gal(β1−6)GlcNAc the response was too low for reliable quantitative data to be derived. In addition to binding parameters, SPR results provided helpful structural insights into the binding events, particularly about the functional groups involved in each interaction. Thus, binding to ECA was strongly influenced by the type of glycosidic linkage, as well as by the nature of the monosaccharide at the reducing end, with a clear preference for Gal(β1−4)GlcNAc, in agreement with previous studies.[23] For this most favorable epitope, the 15-fold higher affinity over Gal(β1−4)Glc underlines the significant role of the *N*-acetyl group at position C2 in lectin binding. Also, by comparing the responses of the three *N*-acetyl-disaccharides,

dx.doi.org/10.1021/ac300766z | *Anal. Chem.* 2012, 84, 6515−6520

the relative role of the hydroxyls of the nonterminal sugar in the interaction can be ascertained. Thus, the decreased binding of the β1−3 isomer (8% relative to the β1−4), or the even lower affinity of the β1−6-linked disaccharide suggest that both C6 and C3 hydroxyls are significantly involved in the canonic binding of Gal(β1−4)GlcNAc to ECA, so that when either of these hydroxyls is obliged to engage in glycosidic bond formation impaired affinity ensues. In summary, straightforward inspection of SPR data highlights a key role of the *N*-acetyl group and, to a lesser extent, of the C3 and C6 hydroxyls, in sugar−ECA recognition, in good agreement with X-ray data showing the O3, N2, O6, and O_{NAc} atoms to be directly involved in the interaction.[24]

SPR-Derived Thermodynamic Parameters. In addition to the kinetic and structural information discussed above, thermodynamic parameters for the preferential Gal(β1−4)GlcNAc (lacNAc)−ECA interaction could also be determined in real time by monitoring the SPR response at various temperatures. Figure 2 (left) shows ECA binding profiles in the 10 to 25 °C range, and how temperature rise affected (i.e., accelerated) both association and dissociation steps. Both k_a and k_d rate constants were determined at each temperature by locally fitting the sensorgrams to the five concentrations used. The derived association constants (K_A) at each temperature were then used to calculate thermodynamic parameters by means of the Van't Hoff equation:

$$\ln K_A = -\Delta H^\circ/RT + \Delta S^\circ/R$$

where R = 8.314 J K^{-1} mol^{-1}.

Alternatively, thermodynamic parameters could also be determined from each rate constant (k_a, k_d), independently, by means of the Eyring equation

$$\ln(k/T) = -\Delta H/RT + -\Delta S/R + \ln(k'/h)$$

where k is the appropriate rate constant and k' and h are the Boltzmann (k' = 1.380 × 10^{-23} J K^{-1}) and the Planck (h = 6.626 × 10^{-34} J s) constants, respectively.

Both Van't Hoff and Eyring plots (Figure 2 Top right A, B) could be fitted to a linear model. The ΔH values derived from each analysis (−41.9 and −42.3 kJ mol^{-1}, respectively) were in good agreement with the −45.6 and −54.5 kJ mol^{-1} values from ITC and NMR studies, respectively.[25,26]

In all these approaches, entropic values are calculated from the Gibbs free energy equation employing the equilibrium association constant and experimental enthalpy as recommended.[27] The SPR-derived equilibrium constant for lacNAc ($K_A \approx 10^6$ M^{-1} at 25 °C, Figure 2) is about 2 orders of magnitude higher than previously reported ITC- and NMR-derived values for the same disaccharide in free form ($K_A \approx 10^4$ M^{-1}, Figure 2 bottom right). Similar differences between surface- and solution-based methods have been already observed for other carbohydrate−lectin interactions,[28] probably because lectin multivalency in addition to the rather high glycan surface density required for SPR experiments may increase the apparent affinity through secondary interactions. In any event, such differences in equilibrium constants, compounded with the slightly different ΔH values from SPR and ITC/NMR methods, can explain the discrepancy in entropic values found in Figure 2 (bottom right).

SPR Lectin Capture and MALDI-TOF MS Identification. In addition to quantitative kinetic data, SPR can serve as an affinity capture/purification platform allowing subsequent MS identification. This is shown here for the interaction of ECA with Gal(β1−4)GlcNAc, the glycoprobe with the highest affinity. The lectin, a 55 kDa dimer, gave a 790 RU readout, that is, an estimated 790 pg of surface-bound material. This was then specifically eluted with excess disaccharide by means of the instrument's recovery function, devised to retrieve affinity-captured material in a very small (2 μL) volume, separated by air bubbles to avoid sample diffusion or cross-contamination. Concentration by vacuum centrifugation furnished enough material (ca. 15 fmol) for molecular weight determination (Figure 3). In this particular case, the fast dissociation of ECA

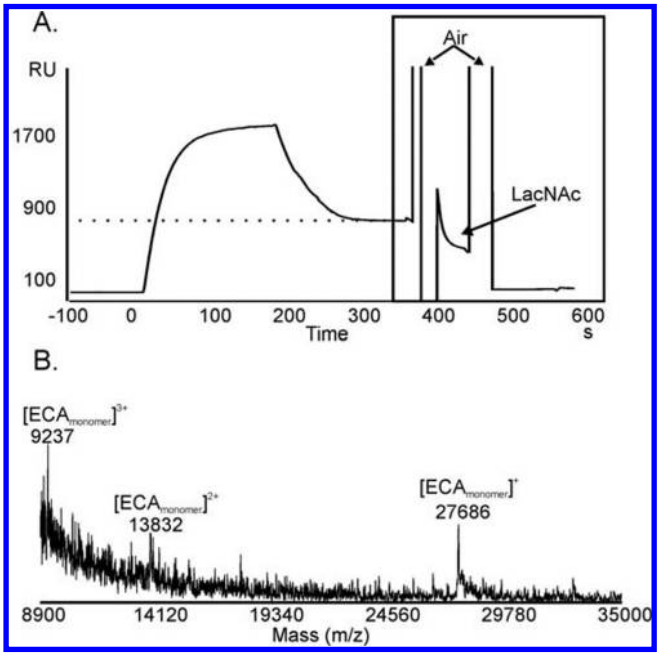

Figure 3. (A) SPR sensorgram of the recovery experiment over lacNAc-glycoprobe. ECA at 1 μM was passed on the glycosylated surface and the captured material (~15 fmol) was recovered with 2 μL lacNAc. (B) MALDI-TOF MS spectrum of the recovered protein.

(k_d = 5.3 × 10^{-3} s^{-1}) complicated recovery and subsequent analysis, compared to other lectins with lower dissociation rates and molecular weights (e.g., wheat-germ agglutinin, data not shown).

In conclusion, the combination of SPR and MALDI-TOF MS molecular weight determination allows successful characterization of sugar−lectin interactions, provided the dissociation rate of the complex and the desorption ability of the lectin are favorable enough.

Carbohydrate-Binding Site Determination by CREDEX-MS. Practically all the current approaches to protein characterization rely on the combined use of proteolysis and MS methods. Direct tryptic digestion of lectin−glycan−*N*[Me]-*O*-Aoa-GFKKG complexes on the SPR chip did not seem advisable, because the Lys residue not used for anchoring the glycoprobe to the chip surface is trypsin-susceptible and cleavage at this site would cause the affinity-bound lectin material to be lost. We therefore opted for off-line proteolysis in a divinylsulfone-based carbohydrate affinity column.[29]

To identify a carbohydrate-binding site by CREDEX-MS, a protease with optimal sequence coverage of the carbohydrate-lectin complex (lacNAc-ECA in our case) is a must. Among three standard proteases, trypsin [1:20 (w:w) ratio] was chosen because it gave 86% coverage (13 peptides, Figure 4A) vs 30% and 26% for chymotrypsin and Glu-C, respectively. Compar-

dx.doi.org/10.1021/ac300766z | *Anal. Chem.* 2012, 84, 6515−6520

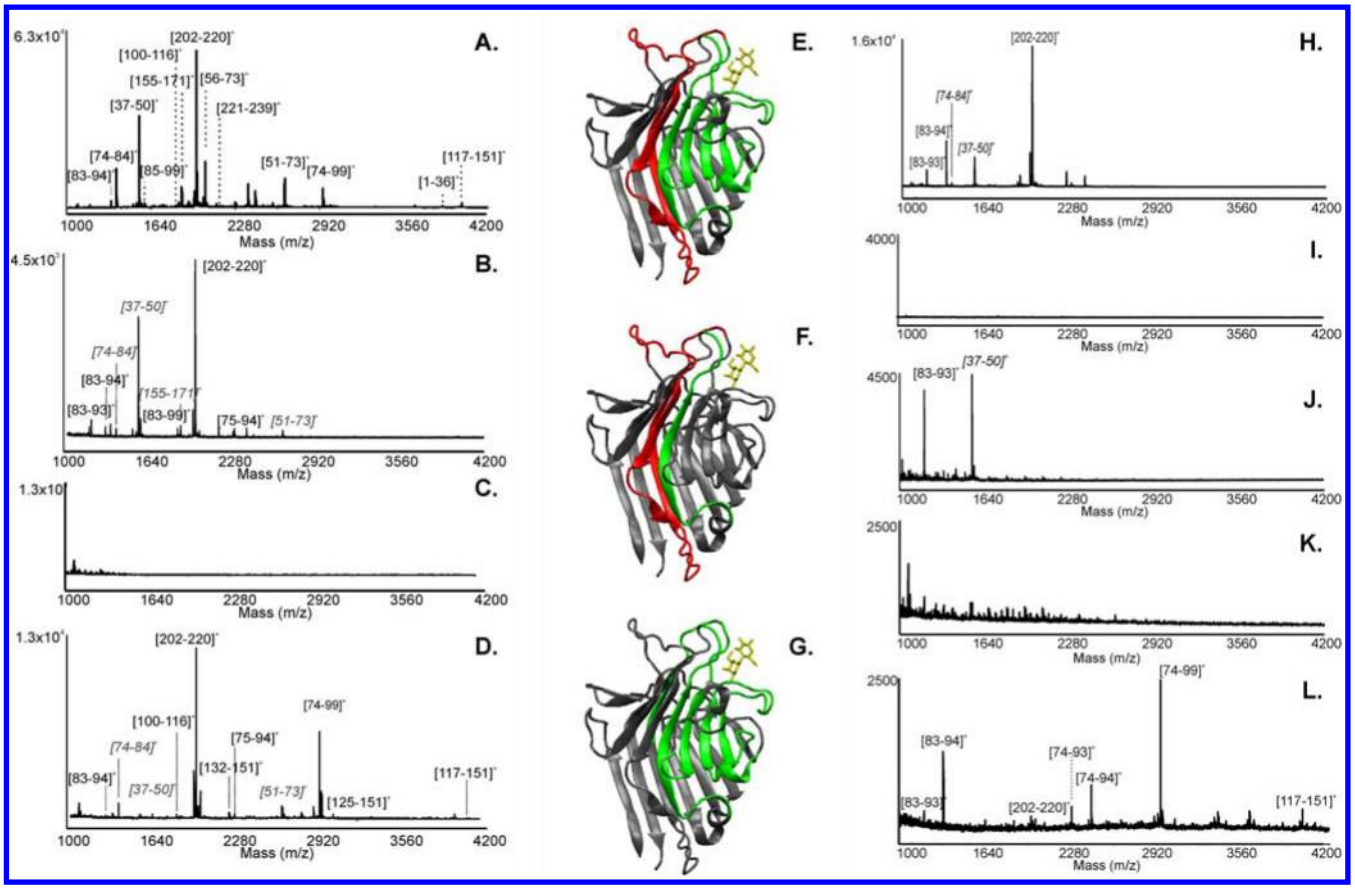

Figure 4. (A) Peptide mass fingerprint of ECA (digestion in solution). (B–D) MALDI-TOF MS spectra corresponding to different fractions of excision experiment. (B) On column digestion with trypsin of the complex lacNAc-ECA. (C) Supernatant after washing. (D) Elution fraction. Peaks in gray show the peptides with no direct contact with the sugar. (Center panel E–G) X-ray crystal structure (PDB 1GZC) of ECA in complex with lactose (in yellow). (E) Peptides identified in the elution fraction of an excision experiment with trypsin are shown in green (sugar-peptide interaction) and red (peptide–peptide interaction) in the ribbon representation. (F) Peptides [37–50], [51–73] and [74–84] (in red), noncovalently bound with spatially close [202–220] (in green), "ride" with this peptide in the elution fraction. (G) In an excision experiment with two consecutive digestions, only peptides involved in sugar-peptide interactions (in green) are detected.[22] (Right panel H–L) MALDI-TOF MS spectra corresponding to different fractions of excision experiment with two consecutive proteolytic digestions. (H) First on column digestion with trypsin of the complex lacNAc-ECA. (I) Supernatant after washing. (J) Second on column digestion with chymotrypsin. (K) Supernatant after washing. (L) Elution fraction.

ison of the standard (Figure 4A) with the flow-through from on-column digest (Figure 4B) revealed essentially identical mass fingerprint peaks with only minor differences in intensity. The column was next washed until no peptide signals were observed (Figure 4C) and then the glycan-interacting peptides were eluted with 60% acetonitrile in water and analyzed (Figure 4D). In this fraction, several peptides {[74–99], [75–94], [83–94], [100–116], [117–151], and [202–220]} (Figure 4D) that contain amino acids displaying direct contact with the carbohydrate in the X-ray structure of the Lac-ECA complex (Figure 4E) could be unequivocally assigned to the binding site. In addition to these specific peptides, three peptides found in low abundance {[37–50], [51–73], and [74–84]} showed no contacts with the sugar in the X-ray structure (Figure 4F); hence no relation to the binding site. Their presence in the elution fraction was explained as a case of "riding" (via β-strand interaction) with the spatially close, glycan-binding peptide [202–220].

To confirm the binding site identification, an additional chymotrypsin digestion subsequent to the trypsin excision was performed. Figure 4 (right panel H–L) shows that, after sequential trypsin-chymotrypsin digestions, the longest peptide [202–220] is split into shorter fragments and the "riding peptides", [37–50], [51–73], and [74–84], are no longer observed in the elution fraction, while the specific binding peptides [74–99], [117–151], as well as nondigested [202–220] remain present (Figure 4L). This result proves that the Gal(β1–4)GlcNAc-ECA interaction can withstand prolonged, sequential digestion with two proteases, despite its relatively low affinity (see Figure 1), hence making possible accurate molecular definition of the interaction partners and removal of unspecific peptides. This is valuable when proteolytic excision results in long peptides enhancing the likelihood of peptide–peptide interactions that may hamper the identification of the carbohydrate binding site.

Additional unequivocal identification of the binding site came from an extraction MS experiment,[20] where ECA was first digested with trypsin, the digest was passed through the affinity column, and only peptides [202–220] and [74–99] representing the binding site were observed (data not shown).

CONCLUSION

Detailed molecular description of carbohydrate–protein interactions is feasible by the combination of analytical

dx.doi.org/10.1021/ac300766z | Anal. Chem. 2012, 84, 6515–6520

techniques described here, which use low amounts of both lectin and carbohydrate compatible with extraction from natural sources, in contrast with more sample-demanding techniques such as NMR or X-ray crystallography. The agglutinin ECA has been chosen as a case study to test the applicability of these techniques. SPR-based experiments showed a higher affinity of ECA for lacNAc relative to other β-galactosides. Additional structural information on the interaction was also provided by SPR, by comparing the differential binding responses between epitopes with subtle differences (i.e., glycosidic linkage or *N*-acetyl group at position C2). This analysis showed the hydroxyls at C3 and C6, as well as the *N*-acetyl at C2, being critical for interaction with ECA. Thermodynamic data on the interaction were also derived by SPR. While enthalpy values were equivalent to those obtained by ITC or NMR, the higher affinity constants determined by SPR translated into larger differences in entropy relative to ITC or NMR. Finally, SPR technology was successfully applied as a lectin capture platform for subsequent MS analysis. SPR-based results are shown to be an efficient combination with CREDEX-MS, which provides a molecular definition of the carbohydrate-binding site. CREDEX-MS in conjunction with the SPR approach described here constitutes a valuable set of tools for decrypting carbohydrate–protein interaction details.

AUTHOR INFORMATION

Corresponding Author

*E-mail: rgutierrez@imim.es (R.G.-G.); david.andreu@upf.edu (D.A); michael.przybylski@uni-konstanz.de (M.P.).

Notes

The authors declare no competing financial interest.

ACKNOWLEDGMENTS

This work was supported by the Spanish Ministry of Science and Innovation (projects BIO2008-04487-CO3-02 and HA2007-0021 to D.A. and BIO2009-08983 to R.G.G., and predoctoral fellowship BES-2006-12879 to C.J.C.), by the Spanish Ministry of Economy and Competitiveness (project SAF2011-24899 to D.A.), and by the Deutsche Forschungsgemeinschaft (PR-175/14-1) and the EU (MSLife).

REFERENCES

(1) Imberty, A.; Varrot, A. *Curr. Opin. Struct. Biol.* **2008**, *18*, 567–576.
(2) Rambaruth, N. D.; Dwek, M. V. *Acta Histochem.* **2011**, *113*, 591–600.
(3) Velasquez, J. G.; Canovas, S.; Barajas, P.; Marcos, J.; Jimenez-Movilla, M.; Gutiérrez-Gallego, R.; Ballesta, J.; Aviles, M.; Coy, P. *Mol. Reprod. Dev.* **2007**, *74*, 617–628.
(4) Apweiler, R.; Hermjakob, H.; Sharon, N. *Biochim. Biophys. Acta* **1999**, *1473*, 4–8.
(5) Puig, O.; Caspary, F.; Rigaut, G.; Rutz, B.; Bouveret, E.; Bragado-Nilsson, E.; Wilm, M.; Seraphin, B. *Methods* **2001**, *24*, 218–229.
(6) Bruckner, A.; Polge, C.; Lentze, N.; Auerbach, D.; Schlattner, U. *Int. J. Mol. Sci.* **2009**, *10*, 2763–2788.
(7) Madeira, A.; Ohman, E.; Nilsson, A.; Sjogren, B.; Andren, P. E.; Svenningsson, P. *Nat. Protoc.* **2009**, *4*, 1023–1037.
(8) Gutiérrez-Gallego, R.; Haseley, S. R.; van Miegem, V. F.; Vliegenthart, J. F.; Kamerling, J. P. *Glycobiology* **2004**, *14*, 373–386.
(9) Slepak, V. Z. *J. Mol. Recognit.* **2000**, *13*, 20–26.
(10) Ahmed, F. E.; Wiley, J. E.; Weidner, D. A.; Bonnerup, C.; Mota, H. *Cancer Genomics Proteomics* **2010**, *7*, 303–309.
(11) Duverger, E.; Frison, N.; Roche, A. C.; Monsigny, M. *Biochimie* **2003**, *85*, 167–79.
(12) Besenicar, M.; Macek, P.; Lakey, J. H.; Anderluh, G. *Chem. Phys. Lipids* **2006**, *141*, 169–178.
(13) Roos, H.; Karlsson, R.; Nilshans, H.; Persson, A. *J. Mol. Recognit.* **1998**, *11*, 204–210.
(14) Zhukov, A.; Schurenberg, M.; Jansson, O.; Areskoug, D.; Buijs, J. *J. Biomol. Tech.* **2004**, *15*, 112–119.
(15) Vila-Perello, M.; Gutiérrez-Gallego, R.; Andreu, D. *ChemBioChem* **2005**, *6*, 1831–1838.
(16) Jimenez-Castells, C.; de la Torre, B. G.; Gutiérrez-Gallego, R.; Andreu, D. *Bioorg. Med. Chem. Lett.* **2007**, *17*, 5155–5158.
(17) Jimenez-Castells, C.; de la Torre, B. G.; Andreu, D.; Gutiérrez-Gallego, R. *Glycoconj. J.* **2008**, *25*, 879–887.
(18) Weis, W. I.; Drickamer, K. *Annu. Rev. Biochem.* **1996**, *65*, 441–473.
(19) Asensio, J. L.; Cañada, F. J.; Bruix, M.; Gonzalez, C.; Khiar, N.; Rodriguez-Romero, A.; Jimenez-Barbero, J. *Glycobiology* **1998**, *8*, 569–577.
(20) Moise, A.; Andre, S.; Eggers, F.; Krzeminski, M.; Przybylski, M.; Gabius, H. J. *J. Am. Chem. Soc.* **2011**, *133*, 14844–14847.
(21) Przybylski, M., Moise, A., Gabius, H. J. Identification Of Ligand Recognition Domains. Patent [PCT/EP2009/003495], 2012, 2010.
(22) Svensson, C.; Teneberg, S.; Nilsson, C. L.; Kjellberg, A.; Schwarz, F. P.; Sharon, N.; Krengel, U. *J. Mol. Biol.* **2002**, *321*, 69–83.
(23) Itakura, Y.; Nakamura-Tsuruta, S.; Kominami, J.; Sharon, N.; Kasai, K.; Hirabayashi, J. *J. Biochem.* **2007**, *142*, 459–469.
(24) Elgavish, S.; Shaanan, B. *J. Mol. Biol.* **1998**, *277*, 917–932.
(25) Gupta, D.; Cho, M.; Cummings, R. D.; Brewer, C. F. *Biochemistry* **1996**, *35*, 15236–15243.
(26) De Boeck, H.; Loontiens, F. G.; Lis, H.; Sharon, N. *Arch. Biochem. Biophys.* **1984**, *234*, 297–304.
(27) Roos, H.; Karlsson, R.; Nilshans, H.; Persson, A. *J. Mol. Recognit.* **1998**, *11*, 204–210.
(28) Critchley, P.; Clarkson, G. J. *Org. Biomol. Chem.* **2003**, *1*, 4148–4159.
(29) Stefanescu, R.; Born, R.; Moise, A.; Ernst, B.; Przybylski, M. *J. Am. Soc. Mass Spectrom.* **2011**, *22*, 148–157.